Design of Kinematic DGPS Filters with Consistent Error Covariance Information

Hyung Keun Lee, Chris Rizos, and Gyu-In Jee

Abstract: Consistent and realistic error covariance information is important for position estimation, error analysis, fault detection, and integer ambiguity resolution for differential GPS. In designing a position domain carrier-smoothed-code filter where incremental carrier phases are used for time-propagation, formulation of consistent error covariance information is not easy due to boundedness and temporal correlation of propagation noises. To provide consistent and correct error covariance information, this paper proposes two recursive filter algorithms based on carrier-smoothed-code techniques: (a) the stepwise optimal position projection filter and (b) the stepwise unbiased position projection filter. A Monte-Carlo simulation result shows that the proposed filter algorithms actually generate consistent error covariance information and the neglection of carrier phase noise induces optimistic error covariance information. It is also shown that the stepwise unbiased position projection filter is attractive since its performance is good and its computational burden is moderate.

Hyung Keun Lee is with the Satellite Navigation & Positioning Group as a Visiting Postdoctoral Fellow, School of Surveying and Spatial Information Systems, University of New South Wales, Sydney, Australia((Tel: 61-2-93854184, Fax: 61-2-93137493, e-mail: hyknlee@unsw.edu.au).

Chris Rizos is with the Satellite Navigation & Positioning Group, School of Surveying and Spatial Information Systems, University of New South Wales, Sydney, Australia (Tel: 61-2-93854205, Fax: 61-2-93137493, e-mail: c.rizos@unsw.edu.au), Corresponding Author.

Gyu-In Jee is with the Department of Electronics Engineering, Konkuk University, Seoul, Korea (Tel: 82-2-452-7407, Fax: 82-2-3437-5235, e-mail:gijee@konkuk.ac.kr).

1 Introduction

To achieve good navigation performance under high-dynamics, a filter usually requires two types of sensors; a sensor with fast output rate for time-propagation and a sensor with slow output rate for measurement update. For this reason, a Global Positioning System (GPS) receiver is usually paired with inertial or dead-reckoning sensors [1-3]. If a vehicle′s movement is fully known in advance, a mathematical model describing the vehicle′s dynamics can completely replace the role of fast-rate sensors. In reality, however, the vehicle′s movement cannot be fully known in advance. If the vehicle′s trajectory is *partially* known and the fast-rate aiding sensors are not available, a stochastic model can marginally replace the function of such sensors. For the reason, the well-known GPS Kalman filter [1-3] implemented within GPS receivers typically use simplified dynamic models representing stationary, constant-speed, or constant-acceleration conditions. The performance of such a GPS Kalman filter is strongly dependent on the consistency between the assumed dynamic model and the receiver′s actual motion. If this consistency condition is not satisfied, the performance of the GPS Kalman filter is significantly degraded.

Unlike other positioning sensors, a GPS receiver provides diverse measurements. This diversity of measurements results in substantial improvement in positioning accuracy and fault detection ability. The improvement in positioning accuracy obtained by eliminating an assumed dynamic model in the range domain was first introduced by [4]. Subsequently, several filters have been proposed to eliminate the need for explicit receiver dynamic models in the position domain. In general, these algorithms use the code measurements for measurement update and the carrier measurements for time-propagation. The two most representative algorithms are the complementary filter proposed by [5] and the phase-connected filter proposed by [6].

In addition to the accuracy, a good navigation filter should also provide a reliable measure of how accurate the position estimates are. Due to this requirement a navigation filter usually

computes an error covariance matrix as a statistical measure. An analysis of previous research [4-7] confirms that a detailed treatment of this topic is hard to find. Since carrier phase noise is much less than pseudorange noise, it is usually neglected or approximated. This neglect of carrier phase noise generates inconsistencies in the error covariance information (as will be seen later). Consistent (and realistic) error covariance information plays an important role in position estimation, fault detection, integer ambiguity resolution, and error analysis of differential GPS.

Extending the conventional carrier-smoothed-code techniques, this paper proposes two position domain filter algorithms: (a) the Stepwise Optimal Position projection Filter (SOPF) and (b) the Stepwise Unbiased Position projection Filter (SUPF). Compared to the conventional carrier-smoothed-code filters, the proposed filters fully consider the complex cross-correlation generated by carrier noises and are computationally efficient since they require minimal four states. Since most of the presented derivation procedure is gain-independent, an extension to other variational algorithm is easy.

2 Design of kinematic filter with consistent error covariance

The pseudoranges and carrier phases measured by a single receiver contain a variety of error sources, including receiver clock bias, thermal noise, satellite clock bias, ionospheric delay, tropospheric delay, and multipath disturbance. If a user′s receiver and a reference receiver are located close by, the common-mode error sources such as the satellite clock bias, ionospheric delay, and tropospheric delay can be effectively eliminated [1-3]. This type of data combination is referred to as *single-differencing*. The multipath error can be effectively detected and mitigated by various other methods [8-14]. The corrected pseudorange $\widetilde{\rho}_{j,k}$ and carrier phase $\widetilde{\phi}_{j,k}$ (assuming the common-mode errors and multipath error have been eliminated) can be modeled as [3]:

$$\widetilde{\rho}_{j,k} = e_{j,k}^{T}(x_{j,k} - x_{u,k}) + b_{u,k} + v_{j,k},\ \ v_{j,k} \sim (0, r_{\rho})$$

$$\tilde{\phi}_{j,k} = e_{j,k}^{T}(x_{j,k} - x_{u,k}) + b_{u,k} + n_{j,k} + \lambda \mathsf{N}_j \ , \ \ n_{j,k} \sim (0, r_\phi) \tag{1}$$

where

$e_{j,k}$: Line Of Sight (LOS) vector from the receiver to the j -th satellite

$x_{j,k}$: Earth-Centered Earth-Fixed (ECEF) position of the j -th satellite

$x_{u,k}$: ECEF receiver position

$b_{u,k}$: receiver clock bias

N_j : unresolved integer ambiguity

$v_{j,k}$, $n_{j,k}$: white noise terms in the code and carrier measurements

r_ρ , r_ϕ : uniform noise strength values of code and carrier measurements

The true state vector X_k considered in this paper is composed of the three-dimensional position sub-vector $x_{u,k}$ and the scalar clock bias $b_{u,k}$:

$$X_k := \begin{bmatrix} x_{u,k} \\ \cdots \\ b_{u,k} \end{bmatrix} \tag{2}$$

The symbols $\overline{X}_k$, $\delta\overline{X}_k$, $\overline{P}_k$, $\hat{X}_k$, $\delta\hat{X}_k$, and $\hat{P}_k$ will be used to represent the *a priori* state estimate, *a priori* estimation error, *a priori* error covariance matrix, *a posteriori* state estimate, *a posteriori* estimation error, and *a posteriori* error covariance matrix at the k -th step, respectively.

$$\delta\overline{X}_k \sim (O, \overline{P}_k), \qquad \delta\hat{X}_k \sim (O, \hat{P}_k)$$

$$\delta\overline{X}_k := \overline{X}_k - X_k, \qquad \delta\hat{X}_k := \hat{X}_k - X_k$$

$$\delta\overline{X}_k = \begin{bmatrix} \delta\overline{x}_{u,k} \\ \cdots \\ \delta\overline{b}_{u,k} \end{bmatrix}, \qquad \delta\hat{X}_k = \begin{bmatrix} \delta\hat{x}_{u,k} \\ \cdots \\ \delta\hat{b}_{u,k} \end{bmatrix} \quad \overline{X}_k = \begin{bmatrix} \overline{x}_{u,k} \\ \cdots \\ \overline{b}_{u,k} \end{bmatrix} \hat{X}_k = \begin{bmatrix} \hat{x}_{u,k} \\ \cdots \\ \hat{b}_{u,k} \end{bmatrix} \tag{3}$$

The *a priori* estimate $\overline{X}_{k+1}$ of either the SOPF or SUPF at the $(k+1)$ −th step is generated

after the time-propagation that combines the *a posteriori* estimate $\hat{X}_k$ and the incremental carrier phase measurements $\{\widetilde{\phi}_{j,k+1} - \widetilde{\phi}_{j,k}\}$ at the k-th step. The *a posteriori* estimate $\hat{X}_k$ at the $k-$th step is generated by the measurement update at the k-th step, combining both the *a priori* estimate $\overline{X}_k$ and the new code measurements $\{\widetilde{\rho}_{j,k}\}$ at the k-th step. As will be seen later, between the proposed SOPF and SUPF, the differences arise only in the gain matrix formulation for time-propagation. Thus, two filters are derived at the same time. If it is necessary to discriminate the variables of the two different filters, the superscripts o and s are used to denote the SOPF and SUPF, respectively.

2.1 Measurement update by pseudoranges

The indirect measurement $z_{j,k}$ with respect to $\delta\overline{X}_k$ for measurement update is formed by the following equation:

$$z_{j,k} = \widetilde{\rho}_{j,k} - e_{j,k}^T (x_{j,k} - \overline{x}_{u,k}) - \overline{b}_{u,k} \tag{4}$$

According to Eqs. (1-4), the indirect measurement z_k^j satisfies the condition:

$$\begin{aligned} z_{j,k} &= h_{j,k}\delta\overline{X}_k + v_{k,j} \\ h_{j,k} &:= [e_{j,k}^T \ \vdots \ -1] \end{aligned} \tag{5}$$

Stacking the indirect measurements $\{z_{j,k}\}_{j=1,2,\cdots,J}$ into a single vector Z_k, one obtains:

$$Z_k = H_k\delta\overline{X}_k + v_k, \ \ v \sim (O_{J\times 1}, r_\rho I_{J\times J}) \tag{6}$$

where

$$Z_k := \begin{bmatrix} z_{1,k} \\ z_{2,k} \\ \vdots \\ z_{J,k} \end{bmatrix}, \quad H_k := \begin{bmatrix} h_{1,k} \\ h_{2,k} \\ \vdots \\ h_{J,k} \end{bmatrix}, \quad v_k := \begin{bmatrix} v_{1,k} \\ v_{2,k} \\ \vdots \\ v_{J,k} \end{bmatrix}. \tag{7}$$

Assuming a gain matrix K_k, the *a priori* estimate $\overline{X}_k$ is updated to the *a posteriori* estimate

$\hat{X}_k$ as follows:

$$\hat{X}_k = \overline{X}_k - K_k Z_k \tag{8}$$

Accordingly, the estimation error is updated by Eqs. (1), (3), and (8):

$$\delta\hat{X}_k = \left(I_{4\times 4} - K_k H_k\right)\delta\overline{X}_k - K_k v_k \tag{9}$$

2.2 Time-propagation by incremental carrier phases

To derive the exact measurement equation for time-propagation, it is necessary to define the variables $\Delta x_{u,k}$, $\Delta b_{u,k}$, $\Delta x_{j,k}$, and $\Delta e_{j,k}$ as the increments of the user position, user receiver clock bias, the j-th satellite′s position, and the LOS vector from the k-th step to the $(k+1)$-th step, respectively:

$$\Delta x_{u,k} := x_{u,k+1} - x_{u,k}, \quad \Delta b_{u,k} := b_{u,k+1} - b_{u,k}$$

$$\Delta x_{j,k} := x_{j,k+1} - x_{j,k}, \quad \Delta e_{j,k} := e_{j,k+1} - e_{j,k} \tag{10}$$

Then, according to Eqs. (1) and (10), the incremental carrier phase $(\tilde{\phi}_{j,k+1} - \tilde{\phi}_{j,k})$ satisfies the condition:

$$\begin{aligned}\tilde{\phi}_{j,k+1} - \tilde{\phi}_{j,k} &= (e_{j,k} + \Delta e_{j,k})^T (x_{j,k+1} - x_{u,k+1}) + n_{j,k+1} + b_{u,k+1} \\ &\quad - e_{j,k}^T (x_{j,k} - x_{u,k}) - n_{j,k} - b_{u,k} \\ &= -(e_{j,k} + \Delta e_{j,k})^T \Delta x_{u,k} + n_{j,k+1} - n_{j,k} + \Delta b_{u,k} \\ &\quad + e_{j,k}^T \Delta x_{j,k} + \Delta e_{j,k}^T (x_{j,k+1} - x_{u,k}).\end{aligned} \tag{11}$$

If one forms the indirect measurement $\omega_{j,k+1}$ for time-propagation as:

$$\omega_{j,k+1} := e_{j,k}^T \Delta x_{j,k} + \Delta e_{j,k}^T (x_{j,k+1} - \hat{x}_{u,k}) - (\tilde{\phi}_{j,k+1} - \tilde{\phi}_{j,k}), \tag{12}$$

$\omega_{j,k+1}$ satisfies the following relationship according to Eqs. (7) and (10-12):

$$\omega_{j,k+1} = h_{j,k+1} \Delta X_k + w_{j,k+1}, \qquad \Delta X_k = [(\Delta x_{u,k})^T \vdots \Delta b_{u,k}]^T \tag{13}$$

where

$$w_{j,k+1} := -\Delta e_{j,k}^T \delta\hat{x}_{u,k} - n_{j,k+1} + n_{j,k} \tag{14}$$

Stacking $\omega_{j,k+1}$ for all the satellites into a vector Ω_{k+1} yields the following linear equation:

$$\Omega_{k+1} = H_{k+1}\Delta X_k + W_{k+1} \tag{15}$$

where

$$\Omega_{k+1} := \begin{bmatrix} \omega_{1,k+1} \\ \omega_{2,k+1} \\ \vdots \\ \omega_{J,k+1} \end{bmatrix}, \quad W_{k+1} := \begin{bmatrix} w_{1,k+1} \\ w_{2,k+1} \\ \vdots \\ w_{J,k+1} \end{bmatrix}. \tag{16}$$

According to Eqs. (14) and (16), the equivalent measurement noise vector W_{k+1} can further be decomposed as:

$$W_{k+1} = -\Delta H_k \delta\hat{X}_k - n_{k+1} + n_k \tag{17}$$

where

$$\Delta H_k := H_{k+1} - H_k$$

$$n_k := [n_{1,k} \quad n_{2,k} \quad \cdots \quad n_{J,k}]^T \sim (O_{J\times 1}, r_\phi I_{J\times J}). \tag{18}$$

The decomposition of the measurement vector W_{k+1} in Eq. (17) will be used later in deriving the gain matrix for time-propagation. For temporal use, the gain matrix is simply denoted by U_{k+1}. The gain matrix U_{k+1} should satisfy the condition:

$$U_k H_k = I_{4\times 4} \tag{19}$$

for all k in order to prevent biased estimation. By pre-multiplying U_{k+1} to both sides of Eq. (15), an estimate $\overline{\Delta X_k}(\tilde{\phi}_{k+1}, \tilde{\phi}_k, \hat{X}_k)$ of the incremental state ΔX_k can be obtained:

$$\overline{\Delta X_k}(\tilde{\phi}_{k+1}, \tilde{\phi}_k, \hat{X}_k) = U_{k+1}\Omega_{k+1} = \Delta X_k + U_{k+1}W_{k+1}. \tag{20}$$

where

$$\tilde{\phi}_k := [\tilde{\phi}_{1,k} \quad \tilde{\phi}_{2,k} \quad \cdots \quad \tilde{\phi}_{J,k}]^T. \tag{21}$$

Using the estimated incremental state $\overline{\Delta X_k}(\tilde{\phi}_{k+1}, \tilde{\phi}_k, \hat{X}_k)$, the *a posteriori* estimate $\hat{X}_k$ at the

k -th step is propagated in time to the *a priori* estimate $\overline{X}_{k+1}$ at the $(k+1)$ -th step:

$$\overline{X}_{k+1} = \hat{X}_k + \overline{\Delta X_k}(\tilde{\phi}_{k+1}, \tilde{\phi}_k, \hat{X}_k) \tag{22}$$

By utilizing Eqs.(3), (17), (20), and (23), the estimation error is propagated in time:

$$\delta\overline{X}_{k+1} = (I_{4\times4} - U_{k+1}\Delta H_k)\delta\hat{X}_k - U_{k+1}(n_{k+1} - n_k) \tag{23}$$

2.3 Covariance recursion and gain formula

The recursion equations of the *a priori* and *a posteriori* estimation error $\delta\overline{X}_k$ and $\delta\hat{X}_k$ are derived by combining Eqs. (9) and (23) in two different orders as follows:

$$\begin{aligned}
\delta\hat{X}_k &= (I_{4\times4} - K_k H_k)(I_{4\times4} - U_k \Delta H_{k-1})\delta\hat{X}_{k-1} \\
&\quad - (I_{4\times4} - K_k H_k)U_k(n_k - n_{k-1}) - K_k v_k \\
\delta\overline{X}_k &= (I_{4\times4} - U_k \Delta H_{k-1})(I_{4\times4} - K_{k-1} H_{k-1})\delta\overline{X}_{k-1} \\
&\quad - (I_{4\times4} - U_k \Delta H_{k-1})K_{k-1} v_{k-1} - U_k(n_k - n_{k-1})
\end{aligned} \tag{24}$$

As shown in Eq. (24), the *a priori* estimation error $\delta\overline{X}_k$ is independent of the pseudorange noise v_k Thus, the error covariance matrix is updated according to Eqs. (3) and (9):

$$\begin{aligned}
\hat{P}_k &= (I_{4\times4} - K_k H_k)\overline{P}_k(I_{4\times4} - K_k H_k)^T + r_\rho K_k K_k^T \\
K_k &= \overline{P}_k H_k^T (H_k \overline{P}_k H_k^T + r_\rho I_{J\times J})^{-1} = \frac{1}{r_\rho}\hat{P}_k H_k^T
\end{aligned} \tag{25}$$

Since $\delta\hat{X}_{k-1}$ is independent of n_k, as shown in Eq. (24), the following relationship holds:

$$E[\delta\hat{X}_k n_k^T] = -(I_{4\times4} - K_k H_k)U_k, \quad E[\delta\hat{X}_k n_{k+1}^T] = O_{4\times J} \tag{26}$$

Utilizing Eqs. (3), (23), and (26), the error covariance matrix is propagated in time as follows:

$$\begin{aligned}
\overline{P}_{k+1} &= (I_{4\times4} - U_{k+1}\Delta H_k)\hat{P}_k(I_{4\times4} - U_{k+1}\Delta H_k)^T + 2r_\Phi U_{k+1}U_{k+1}^T \\
&\quad - r_\Phi(I_{4\times4} - U_{k+1}\Delta H_k)(I_{4\times4} - K_k H_k)U_k U_{k+1}^T \\
&\quad - r_\Phi U_{k+1}U_k^T(I_{4\times4} - K_k H_k)^T(I_{4\times4} - U_{k+1}\Delta H_k)^T
\end{aligned} \tag{27}$$

The gains for projecting position error to the next time step are derived by the following reason. Since no constraint is desired on receiver movement, the unbiased estimation of the displacement vector ΔX_k at each time step is the most concern for stepwise position

projection in time. According to the classical linear Gaussian estimation theory [7,8], the optimal unbiased estimate $\overline{\Delta X_k^o}$ of ΔX_k in the least-squares sense can be obtained by applying the weighted pseudo inverse U_{k+1}^o to the measurement vector Ω_{k+1}:

$$\overline{\Delta X_k^o} = U_{k+1}^o \Omega_{k+1} \tag{28}$$

where

$$U_{k+1}^o := [H_{k+1}^T (Q_{k+1}^o)^{-1} H_{k+1}]^{-1} H_{k+1}^T (Q_{k+1}^o)^{-1}$$

$$Q_{k+1}^o := E\left[W_{k+1} W_{k+1}^T\right] \tag{29}$$

According to Eqs. (17) and (29), the error covariance matrix Q_{k+1}^o is:

$$\begin{aligned} Q_{k+1}^o &:= E\left[(-\Delta H_k \delta\hat{X}_k^o - n_{k+1} + n_k)(-\Delta H_k \delta\hat{X}_k^o - n_{k+1} + n_k)^T\right] \\ &= \Delta H_k \hat{P}_k^o (\Delta H_k)^T + 2r_\Phi I_{J\times J} + r_\Phi \Delta H_k \left(I_{4\times 4} - K_k^o H_k\right) U_k^o \\ &\quad + r_\Phi (U_k^o)^T \left(I_{4\times 4} - K_k^o H_k\right)^T (\Delta H_k)^T \end{aligned} \tag{30}$$

If computational efficiency is more emphasized than theoretical accuracy, an equally-weighted pseudo inverse matrix U_{k+1}^s can be utilized instead of U_{k+1}^o:

$$\overline{\Delta X_k^s} = U_{k+1}^s \Omega_{k+1} \tag{31}$$

where

$$U_{k+1}^s := [H_{k+1}^T (Q_{k+1}^s)^{-1} H_{k+1}]^{-1} H_{k+1}^T (Q_{k+1}^s)^{-1},$$

$$Q_{k+1}^s = I_{J\times J} \tag{32}$$

Denoting U_{k+1} for both U_{k+1}^o and U_{k+1}^s and Q_{k+1} for both Q_{k+1}^o and Q_{k+1}^s, it can be verified that:

$$\begin{aligned} I_{4\times 4} - U_{k+1}\Delta H_k &= [H_{k+1}^T (Q_{k+1})^{-1} H_{k+1}]^{-1} [H_{k+1}^T (Q_{k+1})^{-1} H_{k+1} - H_{k+1}^T (Q_{k+1})^{-1} \Delta H_k] \\ &= U_{k+1} H_k \end{aligned} \tag{33}$$

Substituting Eqs. (33) into Eqs. (23) and (27), the time-propagation of the estimation error and error covariance matrix of SUPF is simplified as follows:

$$\delta\overline{X}^{s}_{k+1} = U^{s}_{k+1}[H_k \delta\hat{X}_k - (n_{k+1} - n_k)]$$

$$\overline{P}^{s}_{k+1} = U^{s}_{k+1}\left[\left(1 + 2r_\Phi / r_\rho\right)H_k \hat{P}^{s}_{k} H^{T}_{k} - 2r_\Phi H_k (H^{T}_{k} H_k)^{-1} H^{T}_{k} + 2r_\Phi I\right](U^{s}_{k+1})^{T} \quad (34)$$

The derived SOPF and SUPF are summarised in Table 1 and Table 2, where a selection matrix Γ_k is used to consider abrupt satellite inclusions and outages. The selection matrix Γ_k consists of $0'$s and $1'$s where 1 denotes the measurement that is valid at both the k and $(k-1)$-th step, simultaneously. Thus, the selection matrix Γ_k maps from the J-dimensional measurement vector Y_k that considers all the channels to the reduced measurement vector Y^{*}_{k}:

$$Y^{*}_{k} = \Gamma_k Y_k \quad (35)$$

3 Simulation

To investigate the characteristics of the proposed filters a Monte-Carlo simulation has been performed. In the simulation, the GPS Kalman filter where the dynamic model is approximated, the position domain filter where the carrier noises are neglected, and the proposed two filters are compared. For the Monte-Carlo simulation 100 ensembles of error sequences were generated. During each trial of 3600 seconds, satellite outages were assumed to have occurred at both 2261 seconds and 3517 seconds. The simulation configuration is shown in Fig. 1 (the true positions of satellites and receivers are generated to provide true ranges). To consider the amplification of noise by *single-differencing*, the variances of the code and carrier thermal noises are set as $1.5\,m$ and $0.015\,m$, respectively, which is larger than those of a single receiver. The receiver clock bias is generated by a second-order Markov model appropriate for a crystal oscillator [2,3]. A typical profile of clock bias for one simulation trial is depicted in Fig. 2. The trajectory of the moving receiver is shown in Fig. 3 (note the trajectory repeats a straight run of 195 seconds followed by a circular turn of 5 seconds). During each straight run, the velocity is maintained at 10m/sec, and each circular turn generates a centripetal acceleration of 3m/sec^2.

To compare the performance of the five filters, mean values $\{\tilde{m}(k)\}_{k=0,1,2,\cdots,3600}$ and one-sigma values $\{\tilde{\sigma}(k)\}_{k=0,1,2,\cdots,3600}$ of the error distances are computed based on the Monte-Carlo error statistics:

$$\tilde{m}(k) = \frac{1}{\mathrm{N}-1}\sqrt{\left\{\sum_{i=1}^{\mathrm{N}}[\hat{x}(i,k)-x(k)]\right\}^2 + \left\{\sum_{i=1}^{\mathrm{N}}[\hat{y}(i,k)-y(k)]\right\}^2 + \left\{\sum_{i=1}^{\mathrm{N}}[\hat{z}(i,k)-z(k)]\right\}^2},$$

$$\tilde{\sigma}(k) = \frac{1}{\mathrm{N}-1}\sqrt{\sum_{i=1}^{\mathrm{N}}[\hat{x}(i,k)-x(k)]^2 + \sum_{i=1}^{\mathrm{N}}[\hat{y}(i,k)-y(k)]^2 + \sum_{i=1}^{\mathrm{N}}[\hat{z}(i,k)-z(k)]^2}, \qquad (36)$$

where N indicates the number of ensembles, k indicates the time index, $[x(k), y(k), z(k)]$ indicates the true position, and $[\hat{x}(i,k), \hat{y}(i,k), \hat{z}(i,k)]$ indicates the estimated position by the i-th ensemble of data used in the Monte-Carlo simulation. In addition to $\{\tilde{m}(k)\}_{k=0,1,2,\cdots,3600}$ and $\{\tilde{\sigma}(k)\}_{k=0,1,2,\cdots,3600}$, one-sigma values $\{\hat{\sigma}(k)\}_{k=0,1,2,\cdots,3600}$ of error distances based on each filter′s error covariance matrix are also computed from:

$$\hat{\sigma}(k) = \sqrt{p_{xx}(k) + p_{yy}(k) + p_{zz}(k)} \qquad (37)$$

where $[p_{xx}(k), p_{yy}(k), p_{zz}(k)]$ indicates the diagonal elements of the error covariance matrix that correspond to the position errors.

The simulation results are shown in Figs. 4 and 5. In all the graphs, the dashed line indicates the mean values $\{\tilde{m}(k)\}_{k=0,1,2,\cdots,3600}$ based on the Monte-Carlo error statistics, the solid line indicates the one-sigma values $\{\tilde{\sigma}(k)\}_{k=0,1,2,\cdots,3600}$ based on the Monte-Carlo error statistics, and the dotted line indicates the one-sigma values $\{\tilde{\sigma}(k)\}_{k=0,1,2,\cdots,3600}$ based on the filter′s error covariance matrix.

The upper plot of Fig. 4 shows the performance of the conventional GPS Kalman filter based on the constant velocity model. As indicated by the dashed and solid lines, the GPS Kalman filter accumulates large error periodically when the receiver undergoes circular turns during the

Monte-Carlo simulation. The lower plot of Fig. 4 shows the performance of the position domain code-carrier filter where carrier noises are neglected. This filter can be regarded as a variant of the complementary filter in [5] or the carrier-only filter in [7]. As shown by the solid line, the periodic accumulation of large errors does not occur during the circular turns since, unlike the GPS Kalman filter, no assumption was used regarding the receiver dynamics. The abrupt error jumps that appear in the solid line at both 2261 seconds and 3517 seconds are due to satellite outages. The effect of carrier noise neglect ion can be observed by comparing the solid line and the dotted line. The position domain filter that neglects carrier noise, as in the case of the conventional GPS Kalman filter, is optimistic of its position estimates compared to the actual errors. This effect would get worse if the raw L1 carrier phase measurements are replaced by the wide-lane carrier phase measurements due to amplification of carrier phase noise.

All the plots in Fig. 5 show the simulation results of the two proposed filters. In each plot of Fig. 5 it is hard to discriminate between the solid and dotted lines, since they are close to each other. This means that the error covariance matrix generated by each of the proposed two filters is consistent with the Monte-Carlo error statistics. By comparing the upper plot and the lower plot, it can be seen that the performance of the SOPF and SUPF are practically identical, though the SOPF is theoretically superior to the SUPF. Thus it can also be concluded that the SUPF is more attractive between the proposed two filters since its performance is good with viable computation.

4 Conclusion

To provide consistent error covariance matrices for single-differenced GPS data processing, this paper has proposed two filter algorithms based on the carrier-smoothed-code technique: the SOPF and the SUPF. Through simulation it was verified that the GPS Kalman filter is easily biased due to any inconsistency between the assumed dynamic model and the actual receiver

movements. It was also shown that the inconsistency of the error covariance matrix can not be eliminated if the carrier-smoothed-code technique, without considering the effects of carrier noises, is implemented. Finally, it was shown that all the proposed filters provide unbiased estimates with consistent error covariance matrices. Among the proposed two filters the SUPF was more attractive since it is computationally not too complex and its performance is good.

5 References

1 PARKINSON, B., AND AXELAD, P., *Global Positioning System: Theory and Applications*, American Institute of Aeronautics and Astronautics, 1996.

2 BROWN, R.G., AND HWANG, P.Y.C., *Introduction to Random Signals and Applied Kalman Filtering*, John Wiley & Sons, 1997.

3 FARRELL, J.A., AND BATH, M., *The Global Positioning System and Inertial Navigation*, McGraw-Hill, 1998.

4 HATCH, R.R., 'The Synergism of GPS Code and Carrier Measurements', *Proceedings of the Third International Geodetic Symposium on Satellite Doppler Positioning, Vol. II*, February 1982, New Mexico, pp. 1213-1232.

5 HWANG, P.Y.C., AND BROWN, R.G., 'GPS Navigation: Combining Pseudorange with Continuous Carrier Phase Using a Kalman Filter', *Navigation: Journal of The Institute of Navigation,* 1990, **37** (2) pp. 181-196

6 BISNATH, S.B., AND LANGLEY, R.B., 'Precise, Efficient GPS-Based Geometric Tracking of Low Earth Orbiters', *Proceedings of the Institute of Navigation Annual Meeting*, June 1999, Cambridge, Massachusetts, pp. 751-760

7 VAN GRAAS, F., AND LEE, S.W., 'High-Accuracy Differential Positioning for Satellite-Based Systems Without Using Code-Phase Measurements', *Navigation: Journal of The Institute of Navigation*, 1995, **42** (4) pp. 605-618.

8 VAN NEE, R.D.J., 'The Multipath Estimating Delay Lock Loop: Approaching Theoretical

Accuracy Limits', *Proceedings of Position Location and Navigation Symposium*, April 1994, Las Vegas, Nevada, pp. 246 –251.

9 BRAASCH, M.S., 'GPS Multipath Model Validation', *Proceedings of Position Location and Navigation Symposium*, April 1996, Atlanta, GA, pp. 672-678.

10 AXELRAD, P., COMP, C.J., AND MACDORAN, P.F., 'SNR-Based Multipath Error Correction for GPS Differential Phase'*, IEEE Tr. on Aerospace and Electronic Systems*, 1996, **32** (2) pp. 650-660.

11 KEE, C.D., AND PARKINSON, B., 'Calibration of Multipath Errors on GPS Pseudorange Measurements', *Proceedings of the 7th International Technical Meeting of the Satellite Division of The Institute of Navigation*, Sept 1994, Salt Lake City, Utah, pp. 352-362.

12 GEORGIADOU, Y., AND KLEUSBERG, A., 'On Carrier Signal Multipath Effects in Relative GPS Positioning', *Manuscripta Geodaetica*, 1988, **13** (1) pp. 1-8.

13 RAY, J.K., CANNON, M.E., AND FENTON, P., 'GPS code and carrier multipath mitigation using a multiantenna system', *IEEE Tr. on Aerospace and Electronic System*s, 2001, **37** (1) pp. 183-195

14 LEE, H.K., LEE, J.G., AND JEE, G.I., 'An Efficient GPS Receiver Algorithm for Channelwise Multipath Detection and Real-Time Positioning', *Proceedings of the Institute of Navigation 2002 National Technical Meeting*, February 2002, San Diego, CA, pp. 265-276.

Table 1: Stepwise optimal position projection filter

Initialization:

$$H_{k0}^{*} = \Gamma_{k0} H_{k0}$$

$$\hat{X}_{k0}^{o} = E[X_{k0} \mid \Gamma_{k0} \tilde{\rho}_{k0}]$$

$$\hat{P}_{k0}^{o} = r_{\rho}[(H_{k0}^{*})^{T} H_{k0}^{*}]^{-1}$$

Time-Propagation:

$$H_{k+1}^{*} = \Gamma_{k+1} H_{k+1}, \;\; H_{k}^{d} = \Gamma_{k+1} H_{k}, \;\; \Delta H_{k+1}^{*} = H_{k+1}^{*} - H_{k}^{d}, \;\; \Omega_{k+1}^{*} = \Gamma_{k+1} \Omega_{k+1}$$

$$L_{k+1/k} = \Gamma_{k+1} \Gamma_{k}^{T}$$

$$\begin{aligned} Q_{k+1}^{*} = {} & \Delta H_{k+1}^{*} \hat{P}_{k}^{o} (\Delta H_{k+1}^{*})^{T} + 2 r_{\Phi} I_{\pi(k+1)\times\pi(k+1)} \\ & + r_{\Phi} \Delta H_{k+1}^{*} (I_{4\times4} - K_{k}^{o} H_{k}^{*}) U_{k}^{o} L_{k+1/k}^{T} \\ & + r_{\Phi} L_{k+1/k} (U_{k}^{o}) (I_{4\times4} - K_{k}^{o} H_{k}^{*})^{T} (\Delta H_{k+1}^{*})^{T} \end{aligned}$$

$$U_{k+1}^{o} = [(H_{k+1}^{*})^{T} (Q_{k+1}^{*})^{-1} H_{k+1}^{*}]^{-1} (H_{k+1}^{*})^{T} (Q_{k+1}^{*})^{-1}$$

$$\hat{X}_{k}^{o} = \overline{X}_{k}^{o} - K_{k}^{o} Z_{k}^{*}$$

$$\overline{P}_{k+1}^{o} = U_{k+1}^{o} \left\{ H_{k}^{d} \hat{P}_{k}^{o} (H_{k}^{d})^{T} + r_{\Phi} \begin{bmatrix} 2 I_{\pi(k+1)\times\pi(k+1)} - H_{k}^{d} \left(I_{4\times4} - K_{k}^{o} H_{k}^{*}\right) U_{k}^{o} \\ - (U_{k}^{o})^{T} \left(I_{4\times4} - K_{k}^{o} H_{k}^{*}\right)^{T} (H_{k}^{d})^{T} \end{bmatrix} \right\} (U_{k+1}^{o})^{T}$$

Measurement Update:

$$K_{k}^{o} = \overline{P}_{k}^{o} (H_{k}^{*})^{T} [H_{k}^{*} \overline{P}_{k}^{o} (H_{k}^{*})^{T} + r_{\rho} I_{\pi(k)\times\pi(k)}]^{-1}, \;\; Z_{k}^{*} = \Gamma_{k} Z_{k}$$

$$\hat{X}_{k}^{o} = \overline{X}_{k}^{o} - K_{k}^{o} Z_{k}^{*}$$

$$\hat{P}_{k}^{o} = \left(I_{4\times4} - K_{k}^{o} H_{k}^{*}\right) \overline{P}_{k}^{o} \left(I_{4\times4} - K_{k}^{o} H_{k}^{*}\right)^{T} + r_{\rho} K_{k}^{o} (K_{k}^{o})^{T}$$

Table 2: Stepwise unbiased position projection filter

Initialization:

$$H_{k0}^{*} = \Gamma_{k0} H_{k0}$$

$$\hat{X}_{k0}^{s} = E[X_{k0} \mid \Gamma_{k0} \tilde{\rho}_{k0}]$$

$$\hat{P}_{k0}^{s} = r_{\rho}[(H_{k0}^{*})^{T} H_{k0}^{*}]^{-1}$$

Time-Propagation:

$$H_{k+1}^{*} = \Gamma_{k+1} H_{k+1}, \;\; H_{k}^{d} = \Gamma_{k+1} H_{k}, \;\; \Omega_{k+1}^{*} = \Gamma_{k+1} \Omega_{k+1}$$

$$U_{k+1}^{s} = [(H_{k+1}^{*})^{T} H_{k+1}^{*}]^{-1} (H_{k+1}^{*})^{T}$$

$$\overline{X}_{k+1}^{s} = \hat{X}_{k}^{s} + U_{k+1}^{s} \Omega_{k+1}^{*}$$

$$\overline{P}_{k+1}^{s} = U_{k+1}^{s} \left\{ \begin{array}{c} (1 + 2r_{\Phi} / r_{\rho}) H_{k}^{d} \hat{P}_{k}^{s} (H_{k}^{d})^{T} - 2r_{\Phi} H_{k}^{d} [(H_{k}^{d})^{T} H_{k}^{d}]^{-1} H_{k}^{d} \\ + 2r_{\Phi} I_{\pi(k+1) \times \pi(k+1)} \end{array} \right\} (U_{k+1}^{s})^{T}$$

Measurement Update:

$$K_{k}^{s} = \overline{P}_{k}^{s} (H_{k}^{*})^{T} [H_{k}^{*} \overline{P}_{k}^{s} (H_{k}^{*})^{T} + r_{\rho} I_{\pi(k) \times \pi(k)}]^{-1}, \;\; Z_{k}^{*} = \Gamma_{k} Z_{k}$$

$$\hat{X}_{k}^{s} = \overline{X}_{k}^{s} - K_{k}^{s} Z_{k}^{*}$$

$$\hat{P}_{k}^{s} = \left(I_{4 \times 4} - K_{k}^{s} H_{k}^{*} \right) \overline{P}_{k}^{s} \left(I_{4 \times 4} - K_{k}^{s} H_{k}^{*} \right)^{T} + r_{\rho} K_{k}^{s} (K_{k}^{s})^{T}$$

List of Figures

Fig. 1 Simulation configuration

Fig. 2 A clock error profile

Fig. 3 Trajectory of moving receiver

Fig. 4 Performance of GPS Kalman filter and carrier-smoothed-code filter without carrier noise consideration

Fig. 5 Performance of proposed stepwise unbiased position projection filter and optimal position projection filter

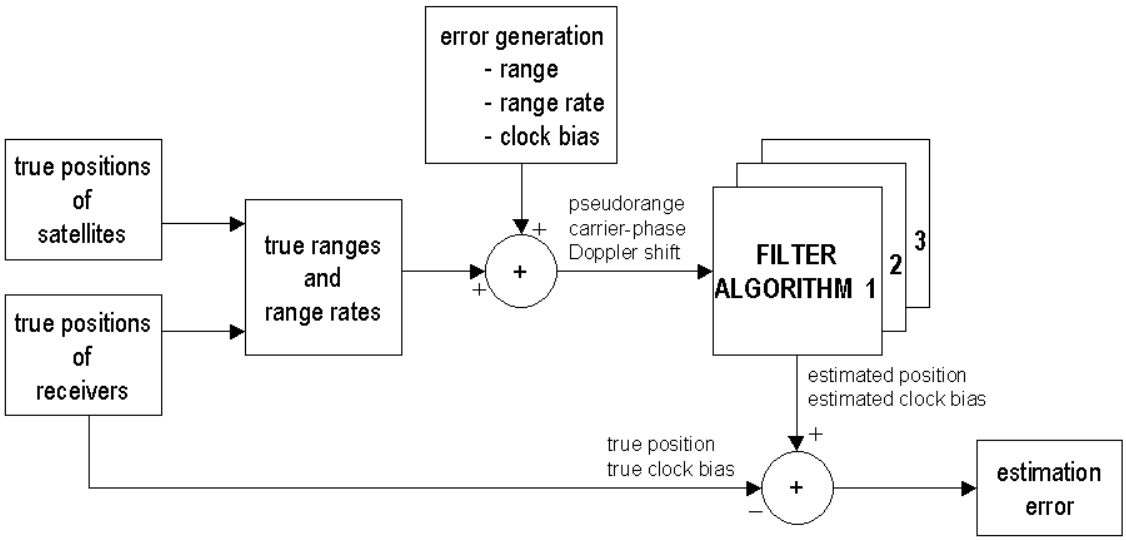

Fig. 1 *Simulation configuration*

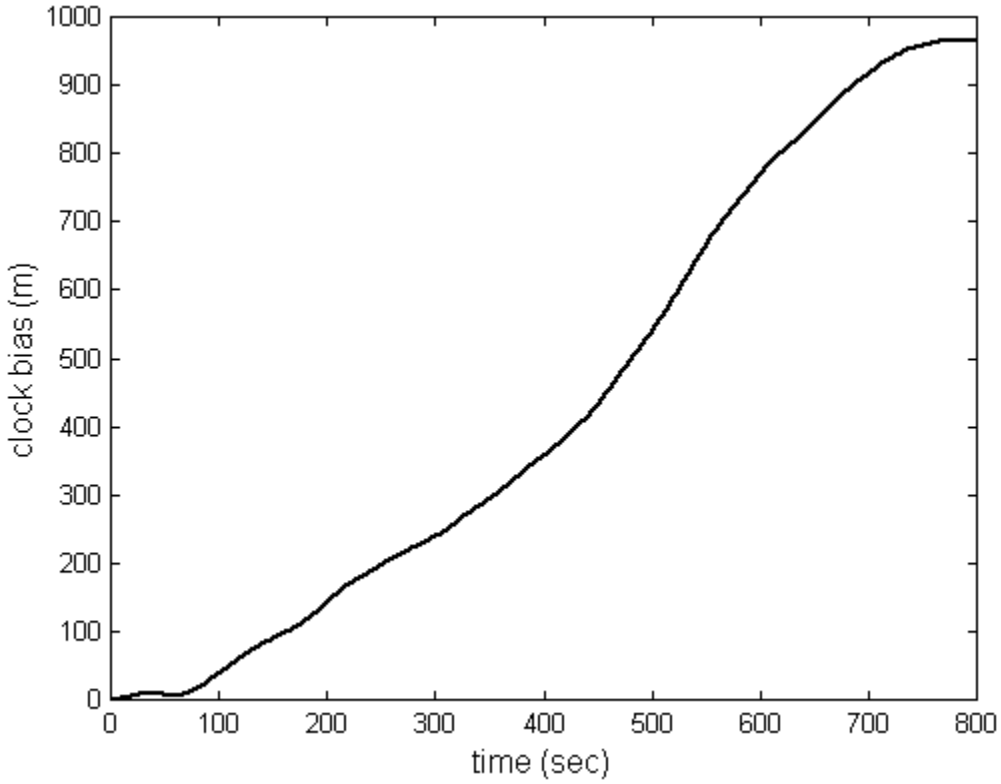

Fig. 2 *A clock error profile*

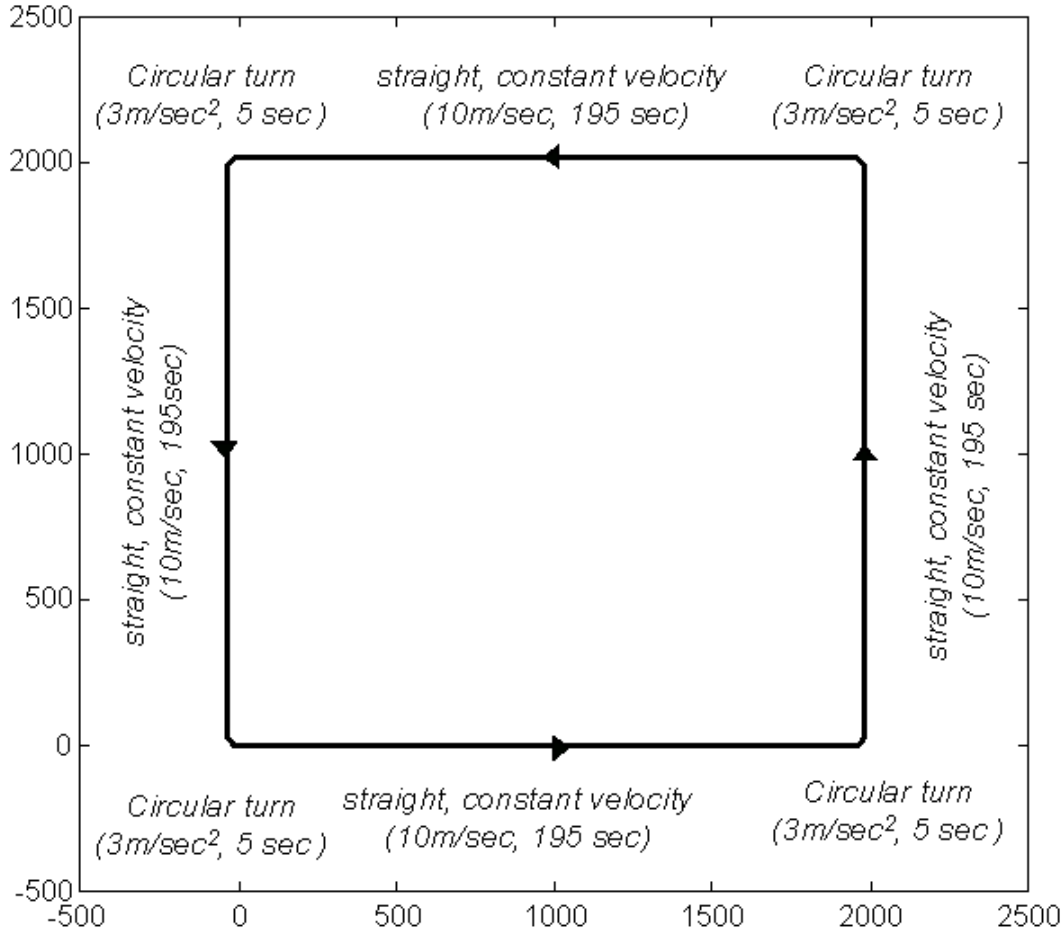

Fig. 3 *Trajectory of moving receiver*

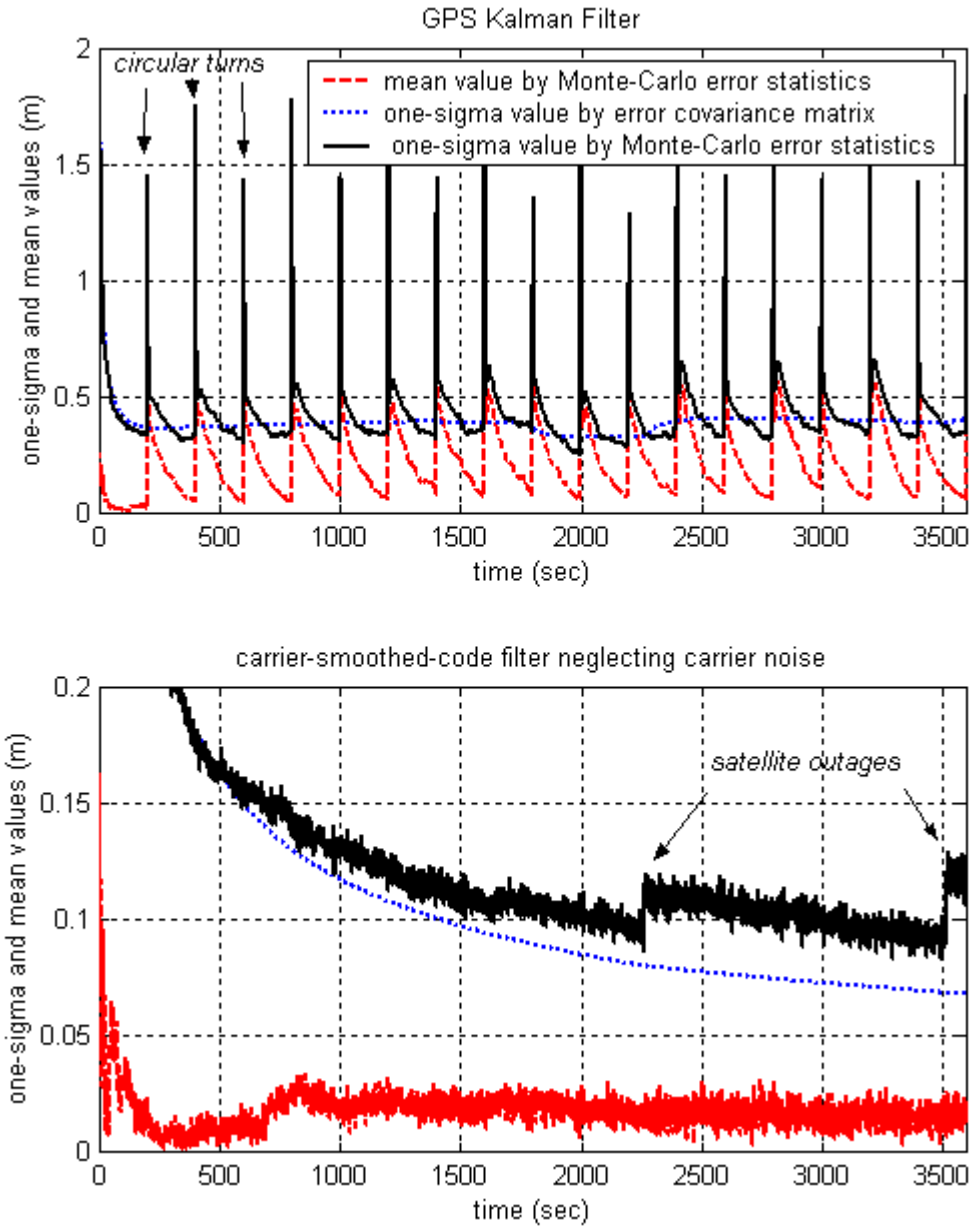

Fig. 4 *Performance of GPS Kalman filter and carrier-smoothed-code filter without carrier noise consideration*

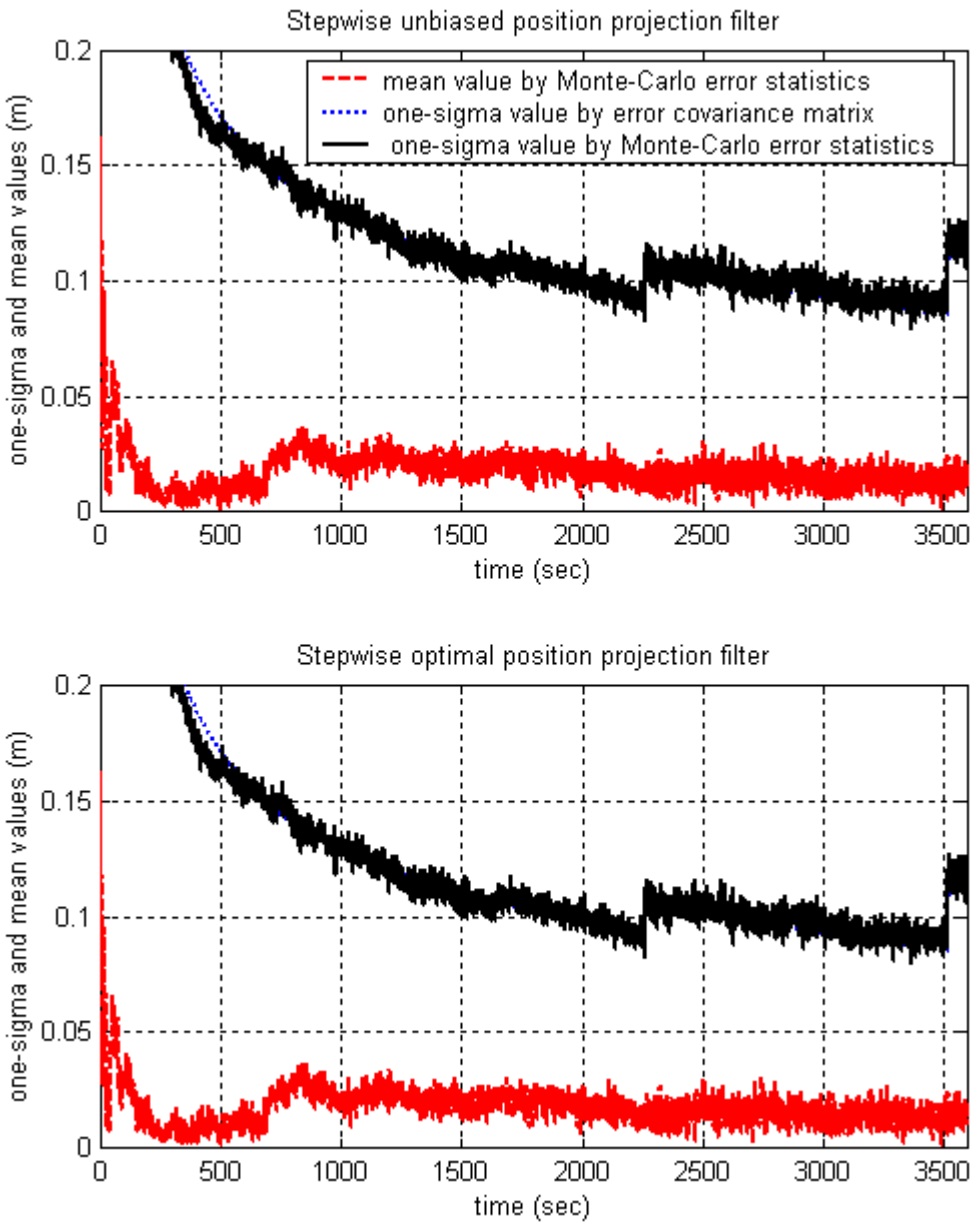

Fig. 5 *Performance of proposed stepwise unbiased position projection filter and optimal position projection filter*